Sensitivity Analysis of Optimum Power Allocation in Sensor Networks that Perform Object Classification

Gholamreza Alirezaei and Rudolf Mathar

***Abstract*—In this paper, we discuss the optimal power allocation in a distributed sensor network for active radar applications. We first determine the behavior of the optimal power strategy with respect to all important system parameters by a simulation set-up. Next, we investigate the sensitivity of the optimal power strategy with respect to an imperfect knowledge of system parameters. We show by simulation results how do different parameter constellations influence the system sensitivity and which parameter is the crucial one for a proper operation of the entire sensor network.**

***Index Terms*—Analytical power allocation, energy-efficient optimization, system sensitivity, network resource management, information fusion.**

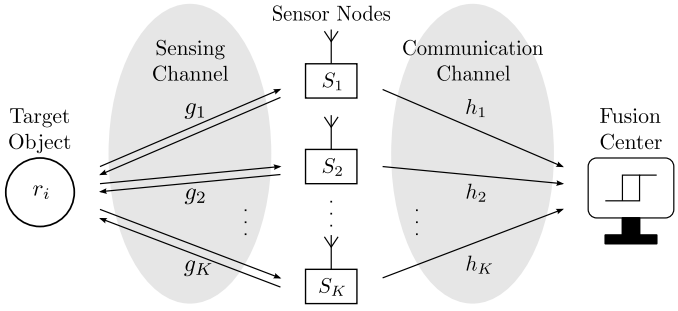

Fig. 1. System model of the distributed wireless sensor network.

I. Introduction

THE research on distributed detection was originated from the attempt to combine signals of different radar devices [Srinivasan, 1986]. Currently, distributed detection is rather discussed in the context of wireless sensor networks, where the sensor units may also be radar nodes [Hume and Baker, 2001; Pescosolido et al., 2008; Yang et al., 2010]. Due to weak batteries and the power-sensitive nature of sensor nodes (SNs), an energy-aware design of the entire network is of high interest. In [Alirezaei and Mathar, 2013b], the power allocation problem for distributed wireless sensor networks, which perform object detection and classification, is only treated for ultra-wide bandwidth (UWB) technology. Other applications, which require or benefit from detection and classification capabilities, are localization and tracking [Gezici et al., 2005] or through-wall surveillance [Debes et al., 2010].

The optimal power allocation for sensor networks, which are used for active radar applications, has been recently investigated analytically in [Alirezaei and Mathar, 2013a] and subsequently extended in [Alirezaei and Mathar, 2014], both for the region of high SNR. The proposed solution in [Alirezaei and Mathar, 2014] includes a total power limitation for the entire sensor network, an individual power limitation for each sensor node, and the combination of both aforementioned types of power limitations. Since the main content of [Alirezaei and Mathar, 2013a] and [Alirezaei and Mathar, 2014] targets at finding a theoretical solution in closed-form to the power allocation problem, it ignores the practical limitations regarding an imperfect channel-state knowledge. In the present paper, we aim to study the behavior of the optimal power allocation from [Alirezaei and Mathar, 2014] with focus on practical inaccuracies. In particular, we investigate the impact of different system parameters and their influence in case of perfect as well as imperfect knowledge of the channel-state.

The present paper is organized as follows. In the next section, we start with a short description of the underlying technical system of the distributed sensor network, which is depicted in Figure 1. The considered system model is a concise representation of the suggested system in [Alirezaei and Mathar, 2014] including important characteristics. Subsequently, theoretical results from [Alirezaei and Mathar, 2014] are discussed and presented in a suitable form for the current investigation. In Section IV, we present an extensive experimental result investigating the behavior of the suggested optimal design strategy with and without channel inaccuracies. We conclude our investigation and restate the major contribution of the present work in the final section.

Mathematical Notations:

Throughout this paper we denote the sets of natural, integer, real, and complex numbers by $\mathbb{N}$, $\mathbb{Z}$, $\mathbb{R}$, and $\mathbb{C}$, respectively. The imaginary unit is denoted by j. Note that the set of natural numbers does not include the element zero. Moreover, $\mathbb{R}_+$ denotes the set of non-negative real numbers. Furthermore, we use the subset $\mathbb{F}_N \subseteq \mathbb{N}$ which is defined as $\mathbb{F}_N := \{1, \ldots, N\}$ for any given natural number N. We denote the absolute value of a real or complex-valued number z by $|z|$ while the expected value of a random variable v is denoted by $\mathcal{E}[v]$. Moreover, the notation $V^\star$ stands for the optimal value

The material in this paper was presented in part at the IEEE Australasian Telecommunication Networks and Applications Conference [Alirezaei and Mathar, 2013a], Christchurch, New Zealand, November 2013.

Both authors are with the Institute for Theoretical Information Technology, RWTH Aachen University, 52056 Aachen, Germany (e-mail: {alirezaei,mathar}@ti.rwth-aachen.de).

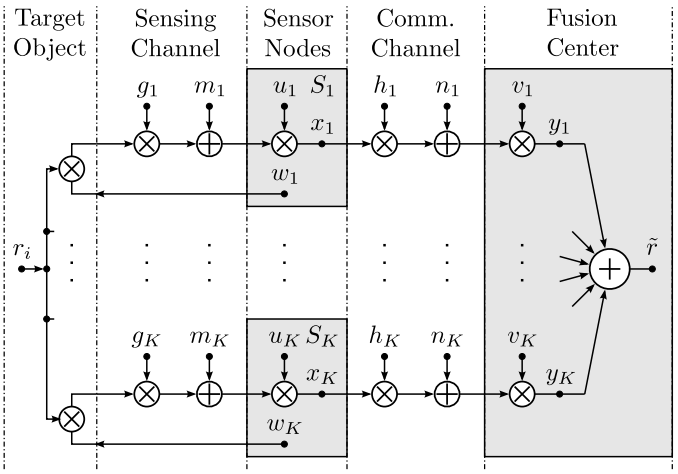

Fig. 2. System model of the distributed active sensor network.

of an optimization variable V at an optimum point of the corresponding optimization problem.

II. Overview and Technical System Description

In the following, we shortly describe the underlying system model that is depicted in Figure 2. A detailed description and specification of the whole system can be found in [Alirezaei and Mathar, 2014]. Hereafter, the continuous-time system is modeled by its discrete-time baseband equivalent, where the sampling rate of the corresponding signals is equal to the target observation rate, for the sake of simplicity. Moreover, we disregard time delays within all transmissions and assume synchronized data communication.

At any instance of time, a network of $K \in \mathbb{N}$ independent and spatially distributed SNs receives random observations. If a target object is present, then the received power at the SN S_k is a part of its own emitted power, which is back-reflected from the jointly observed target object and is weighted by its reflection coefficient $r_i \in \mathbb{C},\ i \in \mathbb{F}_I$, with $r_{\text{rms}}^2 \coloneqq \mathcal{E}[|r_i|^2]$ and $0 < r_{\text{rms}} < \infty$. The object may be of I different types. It should be noted that sheer detection may be treated as the special case of $I = 2$ which corresponds to the decision '*some object is present*' versus '*there is no object*'. We assume that all different object types and their corresponding reflection coefficients are known by the network and the actual target object is assumed to behave static during several consecutive observation steps. Each received signal is in addition weighted by the corresponding channel coefficient $g_k \in \mathbb{C}$ and is disturbed by additive white Gaussian noise (AWGN) $m_k \in \mathbb{C}$ with $M_0 \coloneqq \mathcal{E}[|m_k|^2] < \infty$. We assume that the coherence time of all sensing channels is much longer than the whole length of the classification process. Thus, the expected value and the quadratic mean of each coefficient during each observation step can be assumed to be equal to their instantaneous values, i.e., $\mathcal{E}[g_k] = g_k$ and $\mathcal{E}[|g_k|^2] = |g_k|^2$. Furthermore, the channel coefficients as well as the disturbances are assumed to be pairwise uncorrelated and jointly independent. The sensing channel is obviously wireless.

We model each SN by an amplify-and-forward unit with extended capabilities, where both sensing and communication signals are transmitted simultaneously. The sensing signal w_k, without loss of generality, is assumed to be non-negative, real-valued and deterministic. The expected value of its instantaneous power is then described by

$$W_k \coloneqq \mathcal{E}[|w_k|^2] = |w_k|^2\,,\ k \in \mathbb{F}_K\,. \tag{1}$$

Note that the specific value of w_k is adjustable and will be determined later by the power allocation procedure.

The ratio of the communication signal to the received sensing signal is described by the non-negative real-valued amplification factor u_k which is assumed to be constant over the whole bandwidth and power-range. Thus, the communication signal and the expected value of its instantaneous power are described by

$$x_k \coloneqq (r_i g_k w_k + m_k)u_k\,,\ k \in \mathbb{F}_K \tag{2}$$

and

$$X_k \coloneqq \mathcal{E}[|x_k|^2] = (r_{\text{rms}}^2|g_k|^2 W_k + M_0)u_k^2\,,\ k \in \mathbb{F}_K\,, \tag{3}$$

respectively. The amplification factor is an adjustable parameter and will be determined later by the power allocation procedure, as well. Note that the instantaneous power fluctuates from observation to observation depending on the present target object.

In order to solve the power allocation problem and make a closed-form solution amenable, we assume that the noise power M_0 from (3) is in comparison to $r_{\text{rms}}^2|g_k|^2 W_k$ negligible. This is the case only for the region of high SNR. Thus, we only will consider the useful power

$$X_k \simeq r_{\text{rms}}^2|g_k|^2 W_k u_k^2\,,\ k \in \mathbb{F}_K\,, \tag{4}$$

instead of (3) in what follows.

If the received signal is negligible in comparison to the output signal and if the nodes have smart power components with low-power dissipation loss, then the average power consumption of each node is approximately equal to its average output power $W_k + X_k$. The addition of both transmission powers is justified because the corresponding signals are assumed to be separated by distinct waveforms. We also assume that the output power-range of each SN is limited by P_{max} and that the average power consumption of all SNs together is limited by the sum-power constraint P_{tot}. Hence, the constraints

$$W_k + X_k \le P_{\text{max}} \ \Leftrightarrow\ \big(1 + r_{\text{rms}}^2|g_k|^2 u_k^2\big)W_k \le P_{\text{max}}\,,\ k \in \mathbb{F}_K \tag{5}$$

and

$$\sum_{k=1}^{K} \underbrace{\underbrace{W_k}_{\text{Radar task}} + \underbrace{X_k}_{\text{Data communication}}}_{\text{Average transmission power of one sensor for a single observation}} \le P_{\text{tot}}$$

$$\Leftrightarrow \quad \sum_{k=1}^{K}\big(1 + r_{\text{rms}}^2|g_k|^2 u_k^2\big)W_k \le P_{\text{tot}} \tag{6}$$

arise consequently. We remark that the described method can also be extended to individual output power-range constraints

per SN. Note that the sum-power constraint P_{tot} is a requirement to compare energy-efficient radar systems.

After amplification of the received sensing signal, all local observations are then transmitted to a fusion center, which is placed in a remote location. The communication to the fusion center is performed by using distinct waveforms for each SN so as to distinguish the communication of different SNs. Each waveform has to be suitably chosen in order to suppress inter-user (inter-node) interference at the fusion center. Hence, all K received signals at the fusion center are pairwise uncorrelated and are assumed to be conditionally independent. Each received signal at the fusion center is also weighted by the corresponding channel coefficient $h_k \in \mathbb{C}$ and is disturbed by additive white Gaussian noise $n_k \in \mathbb{C}$ with $N_0 \coloneqq \mathcal{E}[|n_k|^2] < \infty$, as well. We also assume that the coherence time of all communication channels is much longer than the whole length of the classification process. Thus, the expected value and the quadratic mean of each coefficient during each observation step can be assumed to be equal to their instantaneous values, i.e., $\mathcal{E}[h_k] = h_k$ and $\mathcal{E}[|h_k|^2] = |h_k|^2$. Furthermore, the channel coefficients as well as the disturbances are assumed to be pairwise uncorrelated and jointly independent. The data communication between each SN and the fusion center can either be wireless or wired.

The noisy received signals at the fusion center are weighted by $v_k \in \mathbb{C}$ and combined together in order to obtain a single reliable observation $\tilde{r}$ of the reflection coefficient r_i of the actual target object. In this way, we obtain

$$y_k \coloneqq (x_k h_k + n_k) v_k \,, \;\; k \in \mathbb{F}_K \,, \tag{7}$$

and hence,

$$\tilde{r} \coloneqq \sum_{k=1}^{K} y_k = r_i \sum_{k=1}^{K} w_k g_k u_k h_k v_k + \sum_{k=1}^{K} (m_k u_k h_k + n_k) v_k \,. \tag{8}$$

Note that each weight can be written as $v_k = |v_k| \exp(\mathrm{j}\,\vartheta_k)$, $k \in \mathbb{F}_K$, where ϑ_k is a real-valued number which represents the phase of the corresponding weight.

Note that the fusion center can separate all input streams because the data communication is either wired or performed by distinct waveforms for each SN. Consequently, if the communication channel is wireless then a matched-filter bank is essential at the input of the fusion center to separate data streams of different SNs. In addition, we do not consider inter-user (inter-node) interferences at the fusion center because of the distinct waveform choices.

In order to obtain a single reliable observation at the fusion center, the value $\tilde{r}$ should be a good estimate for the present reflection coefficient r_i. Thus, we optimize the sensing power W_k, the amplification factors u_k, and the weights v_k in order to minimize the average absolute deviation between $\tilde{r}$ and the true reflection coefficient r_i. This optimization and its solution are elaborately explained in the next section. After determining the optimal values for W_k, u_k and v_k, the fusion center observes a disturbed version of the true reflection coefficient r_i at the input of its decision unit. Hence, by using the present system model, we are able to separate the power allocation problem from the classification problem and optimize both independently.

TABLE I
NOTATION OF SYMBOLS THAT ARE NEEDED FOR THE DESCRIPTION OF EACH OBSERVATION PROCESS.

Notation	Description
K	number of all nodes;
$\mathbb{F}_K$	the index-set of K nodes;
$\tilde{K}$	number of all active nodes;
I	number of different reflection coefficients;
r_i	reflection coefficient of i^{th} target object;
r_{rms}	root mean squared absolute value of reflection coefficients;
$\tilde{r}$	estimate of the actual reflection coefficient r_i;
g_k, h_k	complex-valued channel coefficients;
m_k, n_k	complex-valued zero-mean AWGN;
M_0, N_0	variances of m_k and n_k;
u_k, v_k	non-negative amplification factors and complex-valued weights;
ϑ_k	phase of v_k;
ϕ_k	phase of the product $g_k h_k$;
w_k, x_k	sensing and communication signal of k^{th} sensor node;
W_k, X_k	sensing and communication power of k^{th} sensor node;
y_k	input signals of the combiner;
P_{max}	output power-range constraint of each sensor node;
P_{tot}	sum-power constraint.

A. Some remarks on the system model

All described assumptions are necessary to obtain a framework suitable for analyzing the power allocation problem, without studying detection, classification and estimation problems in specific systems and their settings.

The accurate estimation of all channel coefficients is necessary for both the radar process and the power allocation. Sometimes it is not possible to estimate the transmission channels; consequently the channel coefficients g_k and h_k remain unknown. In such cases, the radar usually fails to perform its task.

Moreover, since the coherence time of communication channels as well as sensing channels is assumed to be much longer than the whole length of the classification process, the proposed power allocation method is applicable only for scenarios with slow-fading channels.

Note that only the linear fusion rule together with the proposed objective function enable optimizing the power allocation in closed-form. The optimization of power allocation in other cases is in general hardly amenable analytically.

In order to increase the available power-range at each SN, time-division multiple-access (TDMA) can be used to completely separate the sensing task from the communication task and perform each task in a different time slot.

In order to distinguish the current operating mode of each SN in what follows, we say a SN is *inactive* or *idle* if the allocated power is zero. We say a SN is *active* if the allocated power is positive. Finally, we say a SN is *saturated* if the limitation of its output power-range is equal to the allocated power, i.e., $P_{\text{max}} = W_k + X_k$.

An overview of all notations that we will use hereinafter and are needed for the description of each observation process is depicted in Table I.

III. Power Allocation

In this section, we introduce the power optimization problem and present its optimal solution from [Alirezaei and Mathar, 2014] in a concise form. Two different power constraints are simultaneously considered, a sum-power constraint $P_{\text{tot}} \in \mathbb{R}_+$ for the cumulative sum of the expected power consumption of each SN as well as a limitation of the average transmission power of each SN by $P_{\text{max}} \in \mathbb{R}_+$.

In general, the objective is to maximize the overall classification probability, however, a direct solution to the allocation problem does not exist, since no analytical expression for the overall classification probability is available. Instead, we minimize the average deviation between $\tilde{r}$ and r_i, in order to determine the power allocation. The motivation for this method is the separation of the power allocation problem from the object classification procedure, as described in the last section. The corresponding optimization problem is described in the next subsection.

A. Optimization problem

As mentioned in the last section, the value $\tilde{r}$ should be a good estimate for the actual reflection coefficient r_i of the present target object. In particular, we aim at finding estimators $\tilde{r}$ of minimum mean squared error in the class of unbiased estimators for each i.

The estimate $\tilde{r}$ is unbiased simultaneously for each i if $\mathcal{E}[\tilde{r} - r_i] = 0$, i.e., from equation (8) with (1) we obtain the identity

$$\sum_{k=1}^{K} \sqrt{W_k}\, g_k u_k h_k |v_k| \exp(\mathrm{j}\,\vartheta_k) = 1\,. \tag{9}$$

This identity is our first constraint in what follows. Note that the mean of the second sum in (8) vanishes since the noise is zero-mean. Furthermore, we do not consider the impact of both random variables g_k and h_k as well as their estimates in our calculations because the coherence time of both channels is assumed to be much longer than the target observation time.

The objective is to minimize the mean squared error $\mathcal{E}[|\tilde{r} - r_i|^2]$. By using equation (8) and the identity (9) we may write the objective function as

$$V \coloneqq \mathcal{E}\left[|\tilde{r} - r_i|^2\right] = \sum_{k=1}^{K} |v_k|^2 \left(u_k^2 |h_k|^2 M_0 + N_0\right). \tag{10}$$

Note that (10) is only valid if m_k and n_k are white and jointly independent.

As mentioned in the last section, each SN has an output power-range limitation and the expected overall power consumption is also limited. Hence, the objective function is also subject to (5) and (6), which are our second and last constraints, respectively.

In summary, the optimization problem is to minimize the mean squared error in (10) with respect to u_k, v_k, and W_k, subject to constraints (5), (6) and (9).

B. Optimal allocation of power

In the current subsection, we consider the optimization problem from Subsection III-A and highlight corresponding main results from [Alirezaei and Mathar, 2014]. Without loss of generality, we set the useful range of P_{max} and P_{tot} equal to $0 < P_{\text{max}} \leq P_{\text{tot}} \leq K P_{\text{max}}$. By solving the above power optimization problem, a specific quantity for the reliability of each SN is given by

$$c_k \coloneqq \sqrt{\alpha_k} + \sqrt{\beta_k} \;\Rightarrow\; c_k \in \mathbb{R}_+\,, \tag{11}$$

where for the sake of simplicity, both notations

$$\alpha_k \coloneqq \frac{M_0}{r_{\text{rms}}^2 |g_k|^2} \;\Rightarrow\; \alpha_k \in \mathbb{R}_+ \tag{12}$$

and

$$\beta_k \coloneqq \frac{N_0}{|h_k|^2} \;\Rightarrow\; \beta_k \in \mathbb{R}_+ \tag{13}$$

are used. If all SNs are such re-indexed that the inequality chain

$$c_k \leq c_{k+1}\;,\; k \in \mathbb{F}_{K-1}\,, \tag{14}$$

holds, then the most and the least reliable SNs are described by c_1 and c_K, respectively. Since the reliability of the first $\tilde{K}$ SNs, with $\tilde{K} \in \mathbb{N}$ and $1 \leq \tilde{K} \leq K$, is better than that of the remaining ones, only these $\tilde{K}$ SNs are active and participate in sensing and data communication. Each of $\tilde{K} - 1$ SNs receives P_{max} for the sum of its sensing and communication powers while the last SN receives the remaining part of the total power. In conclusion, we infer that

$$W_k^\star = \begin{cases} \frac{P_{\text{max}}\sqrt{\alpha_k}}{c_k} & \text{if } k \in \mathbb{F}_{\tilde{K}-1}\;, \\ \frac{P_{\text{remain}}\sqrt{\alpha_k}}{c_k} & \text{if } k = \tilde{K}\;, \end{cases} \tag{15}$$

and

$$X_k^\star = \begin{cases} \frac{P_{\text{max}}\sqrt{\beta_k}}{c_k} & \text{if } k \in \mathbb{F}_{\tilde{K}-1}\;, \\ \frac{P_{\text{remain}}\sqrt{\beta_k}}{c_k} & \text{if } k = \tilde{K}\;, \end{cases} \tag{16}$$

where the remaining power is defined as

$$P_{\text{remain}} \coloneqq P_{\text{tot}} - (\tilde{K} - 1) P_{\text{max}}\,. \tag{17}$$

The number $\tilde{K}$ of active SNs results from $0 < P_{\text{remain}} \leq P_{\text{max}}$, that must be fulfilled for the last SN, and is given by the smallest integer number for which the inequality

$$\tilde{K} \geq \frac{P_{\text{tot}}}{P_{\text{max}}} \tag{18}$$

holds. In addition, the following equations are obtained for each u_k, V, $|v_k|$ and ϑ_k at the optimum point:

$$u_k^\star = \sqrt{\frac{1}{r_{\text{rms}}\,|h_k g_k|}} \sqrt{\frac{N_0}{M_0}}\;,\; k \in \mathbb{F}_{\tilde{K}}\,, \tag{19}$$

$$V^\star = \begin{cases} \frac{r_{\text{rms}}^2}{P_{\text{tot}}\, c_1^{-2}} & \text{if } \tilde{K} = 1\;, \\ \frac{r_{\text{rms}}^2}{P_{\text{remain}}\, c_{\tilde{K}}^{-2} + P_{\text{max}} \sum_{k=1}^{\tilde{K}-1} c_k^{-2}} & \text{if } \tilde{K} > 1\;, \end{cases} \tag{20}$$

$$|v_k^\star| = \begin{cases} \frac{V^\star}{r_{\text{rms}}} \sqrt{\frac{P_{\max}}{c_k^3 |h_k| \sqrt{N_0}}} & \text{if } k \in \mathbb{F}_{\tilde{K}-1} \ , \\ \frac{V^\star}{r_{\text{rms}}} \sqrt{\frac{P_{\text{remain}}}{c_k^3 |h_k| \sqrt{N_0}}} & \text{if } k = \tilde{K} \ , \end{cases} \tag{21}$$

and

$$\vartheta_k^\star = -\phi_k \ , \ k \in \mathbb{F}_{\tilde{K}} \ , \tag{22}$$

where ϕ_k is the phase of the product $g_k h_k$.

IV. Sensitivity Analysis

In this section, we first simulatively investigate the behavior of the optimal value in (20), with respect to $\sigma_g^2 := \mathcal{E}[|g_k|^2]$, $\sigma_h^2 := \mathcal{E}[|h_k|^2]$, M_0 and N_0. Subsequently, we analyze the sensitivity of a sensor network, which is indeed designed by the optimal power allocation strategy from Subsection III-B, but with an imperfect knowledge about the channel-state. In particular, we investigate different independent cases, where the estimates $\hat{g}_k := g_k + \Delta g_k$ and $\hat{h}_k := h_k + \Delta h_k$ are used instead of g_k and h_k itself, respectively, in order to re-design the sensor network. We compare then the optimal value in (20) of the sensor network with optimal known parameters to the conditional mean square error (MSE)

$$\hat{V} := \mathcal{E}\left[|\tilde{r} - r_i|^2 \mid \Delta g_k, \Delta h_k\right] \tag{23}$$

of the re-designed sensor network with imperfect information. In general, the estimate $\tilde{r}$ in (23) is biased compared to the case with perfect information, i.e., $\mathcal{E}[\tilde{r} - r_i] \neq 0$. In addition, the selection of most reliable SNs is no longer ensured. Hence, the value in (23) is mostly greater than that of (20), see also the definition (10). Since an analytical comparison seems to be out of reach, we set out to use numerical methods to obtain the sensitivity analysis and visualize corresponding simulation results.

In order to fairly compare all results, we simulate a *reference* curve for each figure. All reference curves are based on the default value of each parameter, see Table II. Unless otherwise stated, we create an additional curve only by changing the value of a single parameter. The specific value of the parameter under consideration is noted in the legend of the corresponding figure. All random processes g_k, h_k, Δg_k, Δh_k, m_k and n_k are randomly generated with zero mean Gaussian distributions in each simulation step. The random process r_i is randomly generated with a uniform distribution on $\{z \in \mathbb{C} \mid |z| \leq 1\}$ in each simulation step. All other parameters are kept constant.

A. Behavior of $V^\star$

In Figure 3, the decreasing property of $V^\star$ with respect to the variance σ_g^2 of all sensing channels is shown. The reason behind the decreasing property is that the whole network observes the target object more reliable in case where the variance of sensing channels is higher. Furthermore, it can be seen that increasing N_0 has an equivalent effect on the objective as decreasing σ_h^2 and vice versa. It is also interesting to note that the objective shows highest sensitivity to the variation of M_0 when the sensing channel is rather weak (small σ_g^2). The observed sensitivity is illustratively reduced for higher variances of the sensing channel. Furthermore, the objective attains a more or less constant value for very high variances of the sensing channel. The reason is that the resulted objective is dominated by the quality of the communication channel when the sensing channel gets stronger.

TABLE II
Default values of all parameters used for each reference curve.

Parameter	Default value
K	10
r_{rms}^2	1/3
σ_g^2	2
σ_h^2	2
$\sigma_{\Delta g}^2$	0
$\sigma_{\Delta h}^2$	0
M_0	2
N_0	2
$P_{\max}$	2
P_{tot}	10
$\Rightarrow$ P_{remain}	0
$\Rightarrow$ $\tilde{K}$	5

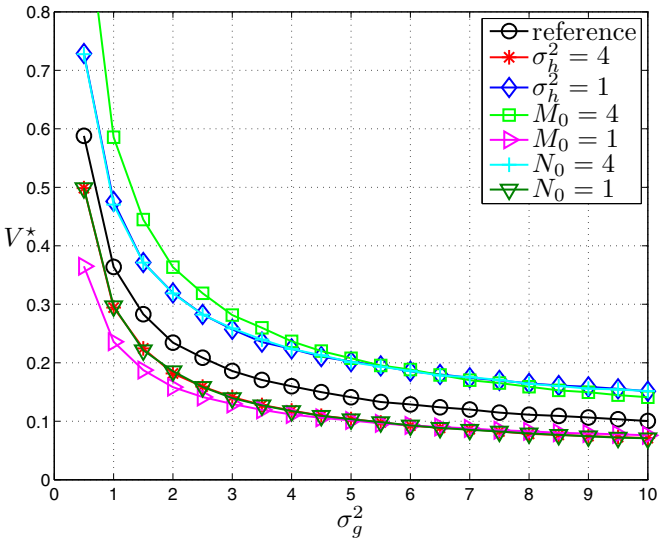

Fig. 3. Behavior of $V^\star$ with respect to σ_g^2. All curves show a decreasing property in σ_g^2. The reference curve has the default parameters $\sigma_h^2 = 2$, $M_0 = 2$ and $N_0 = 2$.

Figure 4 illustrates that $V^\star$ is also decreasing with respect to the variance σ_h^2 of all communication channels. Since the diversity of the communication channel is high for a high value of σ_h^2, the data communication to the fusion center is consequently better which results in a lower $V^\star$. Analogously, increasing M_0 is equivalent to decreasing σ_g^2 and vice versa. Similar to the discussion of the sensing channel, the resulted objective becomes rather constant for a high quality of communication channels, since the sensitivity of the objective is already dominated by the quality of sensing channels and a further improvement of the communication quality is rather unimportant. This also results in a higher sensitivity of $V^\star$ with respect to the sensing quality based on σ_g^2 and M_0 for the region of high σ_h^2.

In Figure 5 it is shown that in contrast to the curves in

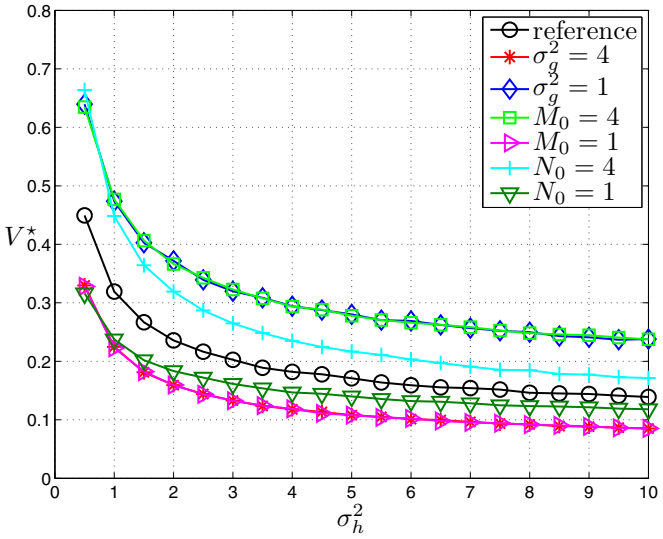

Fig. 4. Behavior of $V^\star$ with respect to σ_h^2. All curves show a decreasing property in σ_h^2. The reference curve has the default parameters $\sigma_g^2 = 2$, $M_0 = 2$ and $N_0 = 2$.

Figure 3 and Figure 4, the property of $V^\star$ is increasing with respect to the noise power M_0. For small values of M_0 all curves have a square root property while for large values of M_0 all curves behave linear. The deviation of all curves is greater for large values of M_0 than for small values. Furthermore, the value of M_0 has more impact on the deviation of $V^\star$ caused by σ_g^2 than by other parameters, as mentioned before. As already described for Figure 3 and Figure 4, increasing N_0 is equivalent to decreasing σ_h^2 and vice versa.

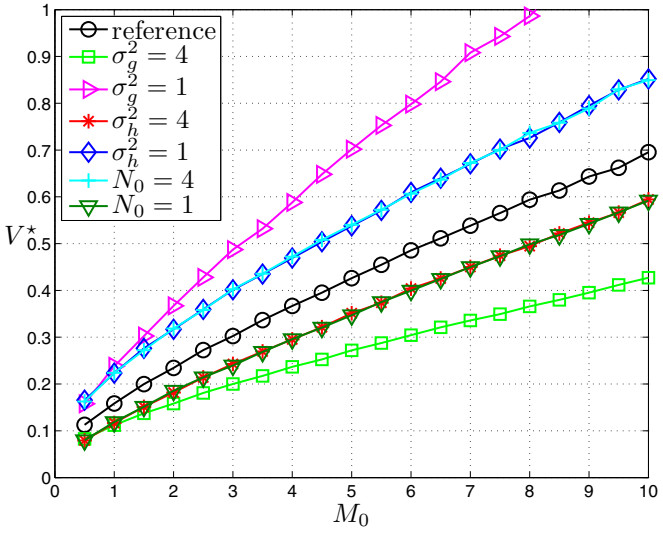

Fig. 5. Behavior of $V^\star$ with respect to M_0. All curves show an increasing property in M_0. The reference curve has the default parameters $\sigma_g^2 = 2$, $\sigma_h^2 = 2$ and $N_0 = 2$.

In Figure 6, the behavior of $V^\star$ is also increasing with respect to the noise power N_0. In general, all curves show a similar behavior compared to those curves in Figure 5.

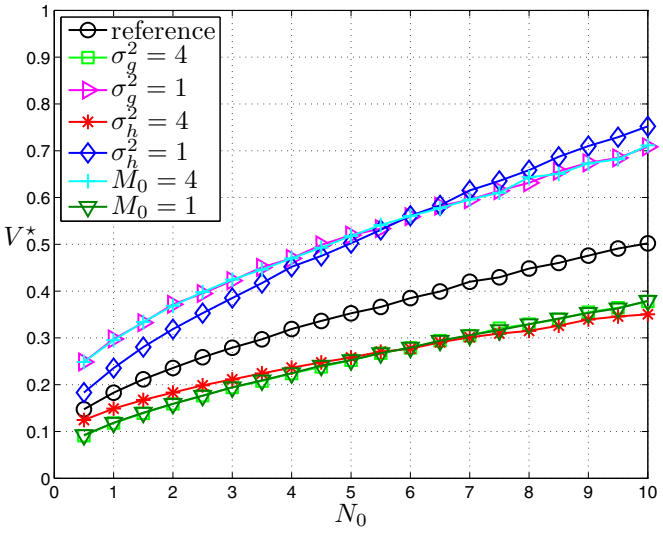

Fig. 6. Behavior of $V^\star$ with respect to N_0. All curves show an increasing property in N_0. The reference curve has the default parameters $\sigma_g^2 = 2$, $\sigma_h^2 = 2$ and $M_0 = 2$.

B. Sensitivity of $\hat{V}$

A sensitivity analysis of $\hat{V}$ is very important in order to justify assumptions concerning the channel-state knowledge. In Figure 7, we consider the case where the error variance $\sigma_{\Delta g}^2 := \mathcal{E}[|\Delta g_k|^2]$ of estimated sensing channels is greater than or equal to zero. In the case where $\sigma_{\Delta g}^2$ is equal to zero, the identity $\hat{V} = V^\star$ holds. Otherwise, $\hat{V}$ is always greater than $V^\star$, i.e., $\hat{V}(\sigma_{\Delta g}^2) \geq \hat{V}(0)$. For high values of $\sigma_{\Delta g}^2$ all curves are linearly increasing. In this region the optimal sensor selection almost always fails. This means that SNs are randomly selected. For low values of $\sigma_{\Delta g}^2$ all curves are rapidly increasing while the correct sensor selection gets out of control. The deterioration of the performance is not only amplified by high noise powers M_0 and N_0, but also by low channel variances σ_g^2 and σ_h^2.

In Figure 8, the other case is depicted in which the estimation of the communication channel is noisy. Analogously, if the variance $\sigma_{\Delta h}^2 := \mathcal{E}[|\Delta h_k|^2]$ of estimation errors is equal to zero, the equality $\hat{V} = V^\star$ holds. In general, all curves again show similar behavior compared to those curves from Figure 7. Interestingly, the curves in Figure 7 achieve mostly a better performance than those in Figure 8. This states that the accurate estimation of all communication channels is more crucial for the system performance than the estimation of sensing channels. The reason behind this fact can be seen from the righthand side of equation (8). An estimation error in each h_k in connection with wrongly optimized u_k and v_k causes additional noises which cannot be caused by an estimation error in each g_k. This asymmetrical property is beneficial, because the estimation of sensing channels is in practice very difficult while the estimation of communication channels can be arbitrarily accurate with the aid of pilot sequences for each SN.

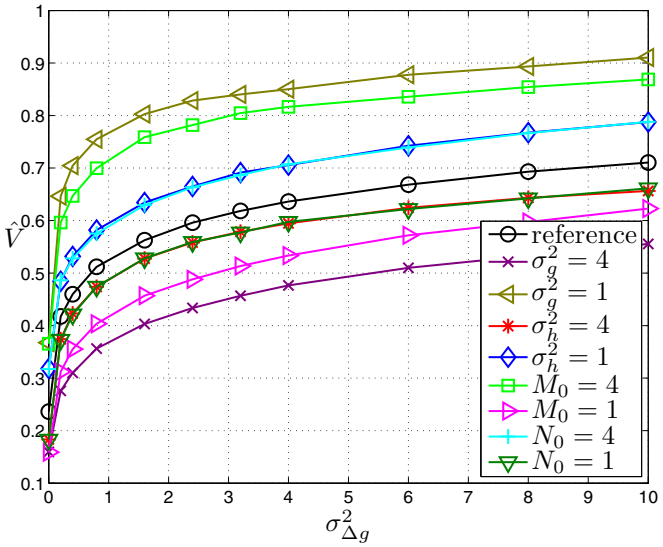

Fig. 7. Behavior of $\hat{V}$ with respect to $\sigma^2_{\Delta g}$. All curves show an increasing property in $\sigma^2_{\Delta g}$. The reference curve has the default parameters $\sigma_g^2 = 2$, $\sigma_h^2 = 2$, $M_0 = 2$ and $N_0 = 2$.

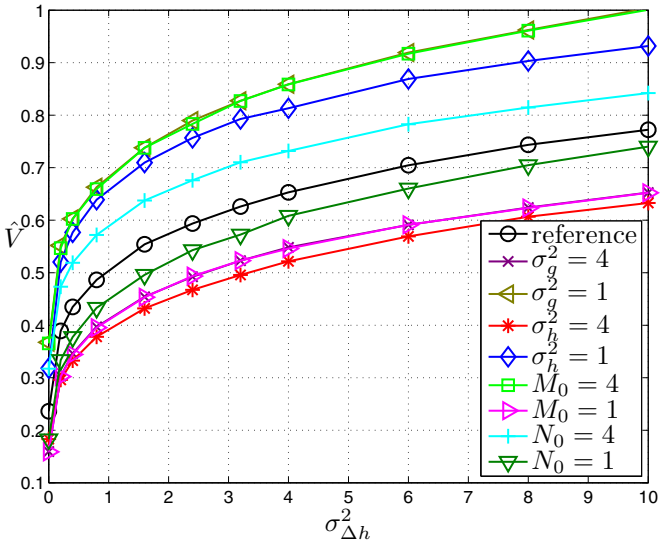

Fig. 8. Behavior of $\hat{V}$ with respect to $\sigma^2_{\Delta h}$. All curves show an increasing property in $\sigma^2_{\Delta h}$. The reference curve has the default parameters $\sigma_g^2 = 2$, $\sigma_h^2 = 2$, $M_0 = 2$ and $N_0 = 2$.

V. Conclusion

The contribution of the present work is to present the sensitivity of the optimal power allocation with respect to the perfect and imperfect knowledge of all important system parameters. Since the sensitivity analysis of the optimal power allocation in an analytical manner seems to be out of reach, we have simulatively investigated the sensitivity. In case of perfect parameter knowledge, the variation of each parameter shows the behavior of the objective with respect to the parameter under consideration. As expected, the objective is decreasing with respect to the variance of channel coefficients and increasing with respect to the variance of noise signals. In case of imperfect channel knowledge, the mean square error is increasing with respect to the variance of estimation errors. All corresponding results show two parts which correspond to the cases '*a selection of more reliable sensor nodes is still feasible*' versus '*the sensor selection is just randomly performed*'. In the latter case, the curves are linearly increasing while in the former case a drastic increase of the curves is visible. Furthermore, the curves demonstrate that an accurate estimation of communication channels is more important in comparison to sensing channels. This property is very crucial for radar systems, since the sensing channel cannot be accurately estimated.

Acknowledgment

This work was assisted by M.Sc. Omid Taghizadeh Motlagh, Institute for Theoretical Information Technology, RWTH Aachen University. We would like to thank him for his effort and commitment. In addition, we would like to thank Prof. Dr. sc. techn. Heinrich Meyr for inspiring us to do the investigation in the present work.

References

G. Alirezaei and R. Mathar, "Optimum power allocation for sensor networks that perform object classification," in *2013 Australasian Telecommunication Networks and Applications Conference (ATNAC 2013)*, Christchurch, New Zealand, Nov. 2013.

——, "Channel capacity related power allocation for distributed sensor networks with application in object classification," in *Computing, Networking and Communications (ICNC), 2013 International Conference on*, 2013, pp. 502–507.

——, "Optimum power allocation for sensor networks that perform object classification," *IEEE Sensors Journal Special Issue on Wireless Sensor Systems for Space and Extreme Environments (WSSSEE)*, 2014, to be published after August 2014.

C. Debes, J. Riedler, A. M. Zoubir, and M. G. Amin, "Adaptive target detection with application to through-the-wall radar imaging," *IEEE Trans. Signal Process.*, vol. 58, no. 11, pp. 5572–5583, 2010.

S. Gezici, Z. Tian, G. B. Giannakis, H. Kobayashi, A. F. Molisch, H. V. Poor, and Z. Sahinoglu, "Localization via ultra-wideband radios: A look at positioning aspects for future sensor networks," *IEEE Signal Process. Mag.*, vol. 22, pp. 70–84, Jul 2005.

A. L. Hume and C. J. Baker, "Netted radar sensing," in *Proc. IEEE Int. Radar Conf.*, 2001, pp. 23–26.

L. Pescosolido, S. Barbarossa, and G. Scutari, "Radar sensor networks with distributed detection capabilities," in *Proc. IEEE Int. Radar Conf.*, May 2008, pp. 1–6.

R. Srinivasan, "Distributed radar detection theory," *IEE Proceedings-F*, vol. 133, no. 1, pp. 55–60, Feb 1986.

Y. Yang, R. S. Blum, and B. M. Sadler, "A distributed and energy-efficient framework for Neyman-Pearson detection of fluctuating signals in large-scale sensor networks," *IEEE J. Sel. Areas Commun.*, vol. 28, pp. 1149–1158, Sep 2010.